Diffusion Tractography of the Corticospinal Tract with Multi-fiber Orientation Filtering

Ryan P. Cabeen, David H. Laidlaw

Computer Science Department
Brown University
Providence, RI, USA
{cabeen,dhl}@cs.brown.edu

Abstract. The reconstruction of the corticospinal tract in the human brain is a clinically important task for both surgical planning and population studies. Diffusion MRI tractography provides an in-vivo and patient-specific technique for mapping the tract's geometry; however, its relationship to other bundles, such as the superior longitudinal fasciculus, presents issues for the standard tensor model, as it cannot represent their crossing fibers. We explore multi-fiber models that have been shown to overcome some of these issues, and evaluate methods for improving on previous work with model-based filtering of orientations. We conduct experiments with real clinical data including normal and tumor-infiltrated corticospinal tracts and compare the single tensor, multi-tensor, and filtered multi-tensor approaches. We found the multi-fiber approach to allow for lateral projections of the tract to be reconstructed and found the addition of orientation filtering to reduce outlier fibers and increase the number of lateral projections. Our results suggest this approach could be considered for clinical applications of corticospinal tract modeling.

Keywords: diffusion MR imaging, white matter, corticospinal tract, multi-fiber models, orientation filtering, model-based image processing

1 Introduction

In this paper, we compare methods for reconstructing the cortico-spinal tract (CST) with diffusion MRI tractoraphy and evaluate the effect of multi-fiber orientation filtering. The reconstruction of the CST is a clinically relevant problem, as an accurate geometric reconstruction can be used both in surgical planning to reduce the risk of unnecessary damage to motor pathways [1] and in neuroimaging population studies. Diffusion tractography provides a tool for extracting patient-specific geometric models of fiber bundles; however, several challenges exist for making this a clinically useful resource for CST reconstruction. First, the anatomy of the CST includes crossings with the superior longitudinal fasciculus (SLF) in the lateral projections [2]. This poses a problem for diffusion models that do not represent complex fiber configurations, such as the single tensor model. Multi-fiber models provide an alternative that theoretically addresses this issue [3], although these can be more difficult to fit numerically and

more susceptible to noise due to the increased number of parameters. A second challenge is the validation for clinical application, which includes establishing the accuracy of the reconstruction with respect to anatomy and the practical value to a clinician. We focus here on the evaluation of methods for tractography, specifically, model-based filtering of multi-fiber models for CST reconstruction. Our goal is for these results to contribute to the larger challenge of validating the use of tractography for clinical applications.

The main contribution of this paper is the application of fiber orientation filtering to the reconstruction of the CST with Extended Streamline Tractography (XST) [3]. Our model-based approach may offer computational and theoretical advantages over image processing performed with the diffusion-weighted images [4]. A number of model-based approaches exist for diffusion imaging, including the Riemannian frameworks for tensors [4], orientation distribution functions [5], and multi-tensor models [6] [7]. In our approach, we apply recent work on model-based processing of multiple orientations [8] and the ball-and-sticks diffusion model [9]. Other methods for orientation regularization have been studied for single [10] [11] [12] and multi-fiber models [13] as well. A related multi-fiber filtering approach developed Kalman filtering for robust model fitting during tractography [14]; however, here we instead process precomputed voxelwise models. Our work distinguishes itself with support on multiple fiber orientations per voxel, an efficient approach, and support for data-adaptive processing similar to a bilateral filter [15].

In the rest of the paper, we conduct experiments testing the quality of corticospinal tract reconstruction with the ball-and-sticks diffusion model. We compare these results with the standard single diffusion tensor model and also test our adaptive orientation filtering approach. We apply this to real clinical brain data including a normal bundle and a bundle infiltrated by metastatic adenocarcinoma. Our findings suggest that the multi-fiber modeling improves the reconstruction of the lateral projections of the CST and that orientation filtering reduces the number of outliers while increasing the number of lateral projections.

2 Methods

In the following sections, we review the diffusion models used in our experiments, describe our tractography algorithm, and present our approach for fiber orientation filtering.

2.1 Diffusion Models

In our analysis, we apply diffusion models supporting both single and multiple fiber per voxel. For single fiber analysis, we use the standard diffusion tensor model, which has the following predicted signal S_i of the i-th diffusion-weighted image (DWI):

$$S_i = S_0 \exp\left(-b_i \boldsymbol{g}_i^T \mathbf{D} \boldsymbol{g}_i\right) \tag{1}$$

given gradient encoding direction $\boldsymbol{g}_i$, b-value b_i, unweighted signal S_0, and diffusion tensor $\mathbf{D}$. We compare this to the multi-fiber ball-and-sticks model, which theoretically can resolve more complex fiber configurations than the single tensor. This is defined by a linear combination of single tensors with the first component being isotropic (ball) and the others being completely anisotropic (sticks). The goal of these constraints is to reduce the number of degrees of freedom while maintaining the ability of the model to reconstruct fiber orientations. The predicted signal S_i of the i-th DWI is as follows:

$$S_i = S_0 \sum_{j=0}^{N} f_j \exp\left(-b_i \boldsymbol{g}_i^T \mathbf{D}_j \boldsymbol{g}_i\right) \tag{2}$$

given N fiber compartments, fiber volume fraction $0 \leq f_j \leq 1$, and $\sum_{j=0}^{M} f_k = 1$. The compartments are then forced to include a completely isotropic first component $\mathbf{D}_0 = \mathrm{diag}(d, d, d)$ and completely anisotropic subsequent components $\mathbf{D}_j = d\boldsymbol{v}_j\boldsymbol{v}_j^T$ with diffusivity d and fiber orientation $\boldsymbol{v}_j$.

2.2 Tractography

We performed tractography using a generalization of the standard streamline approach [16] to account for multiple fibers. In the standard streamline approach, a fiber trajectory is considered a 3D space curve whose tangent vector is equated with the fiber orientation of the voxelwise diffusion models. This can be found by evolving a solution to a differential equation with some initial condition at a given seed position. Typically, some geometric criteria are also used to stop and exclude fibers, including angle threshold and minimum and maximum length. When multiple orientations are present, this approach must be adapted in several ways. First, additional volume fraction termination criteria are included, from the f_i parameters in Eq. 2. During tracking, one of the N possible fiber orientations must also be chosen for the next step. Our approach is similar to Extended Streamline Tractography (XST) [3], although our model does not represent anisotropy in the compartments. The original XST chooses the fiber with the smallest angle difference to the previous step. We take a slightly different approach and randomly choose a fiber among those below a threshold angular difference to the previous step. This seemed to allow tracking in cases where several fibers are quite similar in angular difference to the previous step. Two other issues are interpolation and spatial regularization. The original XST approach interpolates in the DWI image and fits Eq. 2 at each step, but here we test the effect of model-based filtering. A major challenge to a model-based approach is that the presence of multiple fibers per voxel presents a combinatorial problem for matching fibers, which is quite expensive to compute exhaustively even for a small filter support [17]. We address this combinatorial issue with an efficient clustering algorithm and derive estimators for model-based interpolation and filtering, which we describe next.

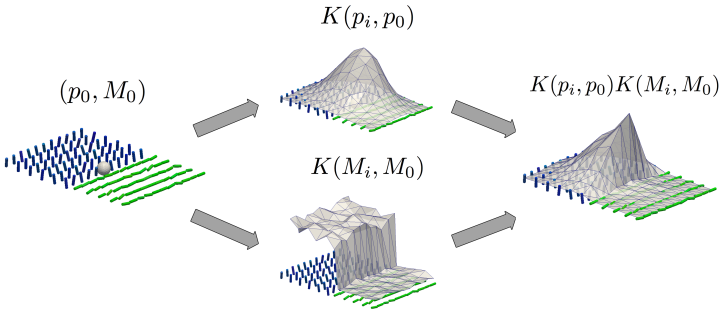

Fig. 1: An illustration of filter weights for a single voxel (left) at a boundary in a noisy phantom. The weights (right) are given by the product of the linear Gaussian (top) and data-adaptive (bottom) weights.

2.3 Orientation Filtering

For the purpose of tractography, we genearalize the diffusion models to include only volume fractions and fiber orientations. We then consider a model M to be a weighted combination of N fiber volume-fraction and orientation pairs $M = \{(f_i, v_i)\}_{i=1}^{N}$ that lie in each voxel. Next, we aim to construct a least squares estimator for fiber models [18] that will provide a way to perform both smoothing and interpolation.

Given an input position p and local neighborhood $\{(p_i, M_i)\}_{i=1}^{C}$ with $M_i = \{(f_{ij}, v_{ij})\}_{j=1}^{N_i}$, the estimator for $\hat{M}$ is given by:

$$\hat{M} = \underset{M}{\operatorname{argmin}} \sum_{i=0}^{C} K\left(\frac{d_e^2(p_i, p)}{h_p^2}\right) d_m^2(M_i, M) \tag{3}$$

given model distance d_m, spatial bandwidth h_p, and kernel function $K(x) = exp(-x)$. We define the model distance between M and $\hat{M}$ by $d_m^2(M, \hat{M}) = \min_\pi \sum_j f_j d_f^2(v_j, \hat{v}_{\pi(j)})$, which is selected across all possible mapping π from fibers in M to $\hat{M}$, with respect to the fiber distance d_f. We then define the fiber distance by the sine of the angle between two fibers a and b: $d_f^2(a, b) = 2(1 - (a \cdot b)^2) = 2sin^2(\theta)$. This was chosen for its theoretical and computational advantages [19] [20] [21] as well as its statistical interpretation [22]. Taken together, the estimator in Eq. 3 can be then expressed by:

$$\hat{M} = \underset{M}{\operatorname{argmin}} \sum_{i}^{C} w_i d_m^2(M_i, M) = \underset{M,\pi}{\operatorname{argmax}} \sum_{i}^{C} \sum_{j}^{N_i} w_i f_{ij} (v_{ij} \cdot v_{\pi(ij)})^2 \tag{4}$$

with weights w_i taken from the above kernel function. For a fixed number of fibers in $\hat{M}$, this objective can be minimized by an iterative Expectation Maximization procedure similar to k-means clustering. In fact, this is equivalent to

the procedure for hard Mixture of Watsons clustering of Sra et al [23] and has been previously applied to linear filtering of multiple orientations [8].

A data-adaptive extension can be obtained by the including a factor for model-to-model similarity in the weights of Eq. 3. This factor is $K\left(\frac{d_m^2(M_i,M_0)}{h_m^2}\right)$, given model bandwidth h_m and reference model M_0. In this case, the weights must be recomputed at each voxel; however, the same EM procedure may be used. An illustration of the data-adaptive filter weights is shown in Fig. 1.

Two additional concerns are the number of fibers and the resulting volume fractions, which we find with a similar estimator for scalar data [18]. The number of fibers is then a weighted average, which is rounded to the nearest integer, and the volume fractions are weighted averages, within groups defined by the optimal fiber correspondences π.

2.4 Bundle Delineation

We used an atlas-based approach [24] to delineate the corticospinal tract with three regions of interest. The diffusion tensor atlas was previously constructed using a population of 80 normal adult subjects [25]. The following three regions were then defined in each hemisphere of the atlas: the posterior limb of the internal capsule, cerebral peduncle, and the precentral brain matter. The first two regions were manually drawn in ITK-SNAP [1] and the precentral region was defined by the population average combined mask of the white and gray matter labels computed with Freesurfer version 5.1 [2]. Visualizations of these regions are shown in Fig. 2. The patient's diffusion tensor volume was then registered to the atlas using deformable tensor-based registration with DTI-TK [3], and the labels were deformed to the patient image space. Tractography seeding was performed in the precentral white matter and only fibers that traversed both other regions were kept.

3 Experiments

Human Brain Data Imaging data of a single patient was downloaded from XNAT [4] as part of the MICCAI 2014 DTI Challenge. The diffusion MRI scans were acquired with a spin-echo EPI sequence with the following parameters: voxel size 2.0 x 2.0 x 2.0 mm, 256 x 256 matrix, 73 slices, b-values 200, 500, 1000 and 3000 s/mm^2, 69 diffusion-weighted volumes and 4 non-diffusion weighted volumes. The patient presented with a metastatic adenocarcinoma infiltrating the corticospinal tract with large edema, both isolated to the right hemisphere.

[1] http://www.itksnap.org/
[2] https://surfer.nmr.mgh.harvard.edu
[3] http://dti-tk.sourceforge.net
[4] http://central.xnat.org

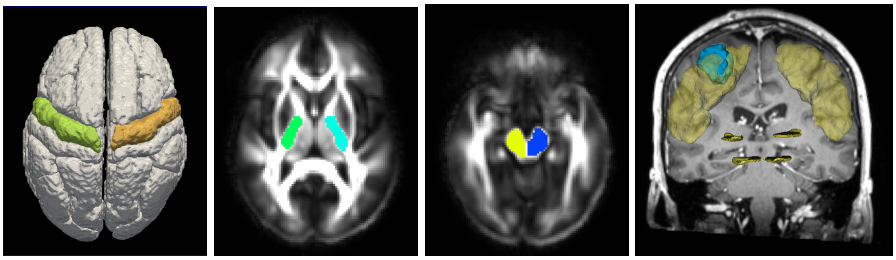

Atlas Precentral Brain Matter	Atlas Posterior Limb of Internal Capsule	Atlas Cerebral Penduncle	Regions deformed from atlas to patient

Fig. 2: Regions of interest used for delineating the corticospinal tract. Atlas space regions are shown in a surface rendering of the superior surface of the precentral brain matter (first), and axial slices of the posterior section of the internal capsule (second) and cerebral peduncle (third). The regions were deformed to patient image space, as shown in a surface rendering (fourth), and used to seed and select fibers in the bundle.

Image Analysis Preprocessing, voxel model fitting, tractography, and visualization were performed as follows. A brain mask was extracted with BET in FSL version 5.0 [5]. Single diffusion tensors were fit with DTIFIT in FSL. Multi-fiber models were fit using an MCMC procedure with XFIBRES in FSL with default parameters. Orientation filtering and interpolation were performed with custom software with $h_p = 3.0$, $h_m = 0.75$, and a filter support of 5 voxels. Tractography was peformed with custom software with the following parameters: angle threshold 50 degrees, step size 1.5 mm, 20 seeds per voxel, minimum length 20 mm, maximum length 110 mm, and volume fraction threshold 0.1. Bundle delineation was performed with custom software, and visualizations were rendered with Slicer [6]. Parameters were chosen by varying them in step-wise fashion.

Results Visualizations in Fig. 3 show the reconstructed bundles. In the left hemisphere, we found the single tensor analysis to be similar to other works [2] and included only the most superior projections. The ball-and-sticks reconstruction improved the tracking through crossing and fanning fibers also similar to previous works [3]. Linear filtering significantly increased the number of lateral projections. The filtering also produced smoother fibers that retained a similar overall shape in the main body of the bundle. The addition of the adaptive term in the filtering added more lateral projections with little other change. The reconstructions in the right hemisphere were significantly different due to the presence of edema and tumor. Only filtered models allowed tracking through some of the edema, and no method tracked through the tumor.

[5] http://www.fmrib.ox.ac.uk/fsl
[6] http://www.slicer.org

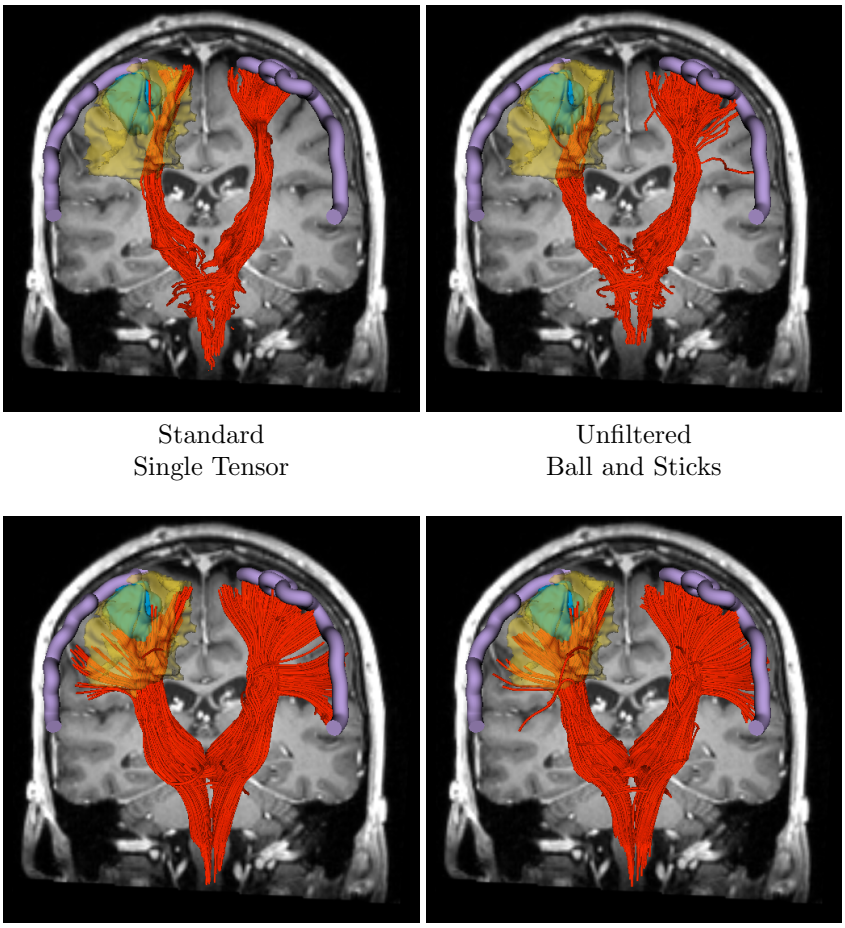

Standard
Single Tensor

Unfiltered
Ball and Sticks

Linear Filtered
Ball and Sticks

Adaptive Filtered
Ball and Sticks

Fig. 3: Tractography (red) for standard single diffusion tensor modeling and ball-and-sticks modeling with and without filtering. Shown are results from standard diffusion tensor (top left), unfiltered ball-and-sticks (top right), linear filtered ball-and-sticks (bottom left), and adaptive filtered ball-and-sticks (bottom right). The outline of motor cortex is overlaid in purple. In the right hemisphere, we see the infiltrating tumor (blue) stops tracking in all models, and the edema (yellow) stops tracking to varying extents. In the left hemisphere, we see that single tensor modeling does not include the lateral projections. Linear filtering increased the number of lateral projections. Adaptive filtering further increased the lateral projections and reduced the number of outlier fibers.

4 Conclusion

In this study, we examined several approaches for the reconstruction of the corticospinal tract and tested the effect of fiber orientation filtering on the quality of the resulting tract geometry. We employed a multi-fiber model to resolve complex fiber configurations at the crossing of the CST with the superior longitudinal fasciculus. Our filtering approach provides an efficient mechanism for both smoothing and interpolation during tractography, and our results suggest that this step aids in tracking the lateral projections to the precentral gyrus. The proposed filtering method could also be applied to other diffusion models that represent multiple fiber orientation. The evaluation of this, as well as a comparison to other approaches such as Kalman filtering, remain open issues. In summary, we found the combination of multi-fiber modeling and orientation filtering to be a valuable approach that could be considered for clinical research applications that aim to understand the structure of the corticospinal tract in both health and disease.

References

1. Coenen, V.A., Krings, T., Axer, H., Weidemann, J., Kränzlein, H., Hans, F.J., Thron, A., Gilsbach, J.M., Rohde, V.: Intraoperative three-dimensional visualization of the pyramidal tract in a neuronavigation system (PTV) reliably predicts true position of principal motor pathways. Surgical Neurology **60**(5) (November 2003) 381–390
2. Kinoshita, M., Yamada, K., Hashimoto, N., Kato, A., Izumoto, S., Baba, T., Maruno, M., Nishimura, T., Yoshimine, T.: Fiber-tracking does not accurately estimate size of fiber bundle in pathological condition: initial neurosurgical experience using neuronavigation and subcortical white matter stimulation. NeuroImage **25**(2) (April 2005) 424–9
3. Qazi, A.A., Radmanesh, A., Donnell, L.O., Kindlmann, G., Whalen, S., Westin, C.f., Golby, A.J.: Resolving crossings in the corticospinal tract by two-tensor streamline tractography. NeuroImage **47** (2010) 1–18
4. Pennec, X., Fillard, P., Ayache, N.: A Riemannian framework for tensor computing. International Journal of Computer Vision **66**(January) (2006) 41–66
5. Goh, a., Lenglet, C., Thompson, P., Vidal, R.: A nonparametric Riemannian framework for processing high angular resolution diffusion images. CVPR (2009)
6. Demiralp, C., Laidlaw, D.H.: Generalizing diffusion tensor model using probabilistic inferenrandom fields. In: Proceedings of MICCAI CDMRI Workshop. (2011)
7. Taquet, M., Scherrer, B., Commowick, O.: A Mathematical Framework for the Registration and Analysis of Multi-Fascicle Models for Population Studies of the Brain Microstructure. IEEE Trans. on Med. Imaging (November 2013) 1–14
8. Cabeen, R.P., Bastin, M.E., Laidlaw, D.H.: Estimating constrained multi-fiber diffusion mr volumes by orientation clustering. In: Medical Image Computing and Computer-Assisted Intervention MICCAI 2013. Volume 8149 of Lecture Notes in Computer Science. (2013) 82–89
9. Behrens, T., Berg, H.J., Jbabdi, S., Rushworth, M., Woolrich, M.: Probabilistic diffusion tractography with multiple fibre orientations: What can we gain? Neuroimage **34**(1) (2007) 144–155

10. Poupon, C., Clark, C., Frouin, V., Régis, J., Bloch, I., Le Bihan, D., Mangin, J.F.: Regularization of Diffusion-Based Direction Maps for the Tracking of Brain White Matter Fascicles. NeuroImage **12**(2) (2000) 184–195
11. Tschumperlé, D., Deriche, R.: Orthonormal vector sets regularization with PDE's and applications. International Journal of Computer Vision **50**(3) (2002) 237–252
12. Coulon, O., Alexander, D., Arridge, S.: Diffusion tensor magnetic resonance image regularization. Medical Image Analysis **8**(1) (March 2004) 47–67
13. Sigurdsson, G., Prince, J.: Smoothing fields of weighted collections with applications to diffusion MRI processing. SPIE Medical Imaging (2014)
14. Malcolm, J.G., Michailovich, O., Bouix, S., Westin, C.F., Shenton, M.E., Rathi, Y.: A filtered approach to neural tractography using the watson directional function. Medical Image Analysis **14**(1) (2010) 58
15. Tomasi, C., Manduchi, R.: Bilateral filtering for gray and color images. In: Computer Vision, Narosa Publishing House (1998) 839–846
16. Basser, P.J., Pajevic, S., Pierpaoli, C., Duda, J., Aldroubi, a.: In vivo fiber tractography using DT-MRI data. Mag. Res. in Med. **44**(4) (October 2000) 625–32
17. Bergmann, O., Kindlmann, G., Peled, S., Westin, C.F.: Two-tensor fiber tractography. In: Biomedical Imaging: From Nano to Macro, 2007. ISBI 2007. 4th IEEE International Symposium on, IEEE (2007) 796–799
18. Takeda, H., Farsiu, S., Milanfar, P.: Kernel regression for image processing and reconstruction. Image Processing, IEEE Transactions on **16**(2) (Feb 2007) 349–366
19. Bhattacharya, R., Patrangenaru, V.: Large Sample Theory of Intrisic Sample Means on Manifolds I. Annals of Statistics **31**(1) (2013) 1–29
20. Knutsson, H.: Representing local structure using tensors. In: Proceedings of the 6th Scandinavian Conference on Image Analysis. (1989)
21. Rieger, B., van Vliet, L.: Representing orientation in n-dimensional spaces. Computer Analysis of Images and Patterns (2003) 1–8
22. Cabeen, R.P., Laidlaw, D.H.: White matter supervoxel segmentation by axial dp-means clustering. In: Medical Computer Vision. Large Data in Medical Imaging. Lecture Notes in Computer Science. (2014) 95–104
23. Sra, S., Jain, P., Dhillon, I.: Modeling data using directional distributions: Part II. Technical Report TR-07-05, Dept. of CS, Univ. of Texas at Austin (2007)
24. Mori, S., Oishi, K., Faria, A.: White matter atlases based on diffusion tensor imaging. Current opinion in neurology **22**(4) (2009) 362–369
25. Cabeen, R.P., Bastin, M.E., Laidlaw, D.H.: A diffusion mri resource of 80 age-varied subjects with neuropsychological and demographic measures. In: ISMRM, 21st Scientific Meeting and Exhibition. Number 2138, Salt Lake City, Utah (2013)